

Loss of *l(3)mbt* leads to acquisition of the ping-pong cycle in *Drosophila* ovarian somatic cells

Tetsutaro Sumiyoshi,^{1,3} Kaoru Sato,^{1,3}
Hitomi Yamamoto,¹ Yuka W. Iwasaki,²
Haruhiko Siomi,² and Mikiko C. Siomi¹

¹Department of Biological Sciences, Graduate School of Science, The University of Tokyo, Tokyo 113-0032, Japan; ²Department of Molecular Biology, Keio University School of Medicine, Tokyo 162-8582, Japan

In *Drosophila* germ cells, PIWI-interacting RNAs (piRNAs) are amplified through a PIWI slicer-dependent feed-forward loop termed the ping-pong cycle, yielding secondary piRNAs. However, the detailed mechanism remains poorly understood, largely because an ex vivo model system amenable to biochemical analyses has not been available. Here, we show that CRISPR-mediated loss of function of *lethal (3) malignant brain tumor [l(3)mbt]* leads to ectopic activation of the germ-specific ping-pong cycle in ovarian somatic cells. Perinuclear foci resembling nuage, the ping-pong center, appeared following *l(3)mbt* mutation. This activation of the ping-pong machinery in cultured cells will greatly facilitate elucidation of the mechanism underlying secondary piRNA biogenesis in *Drosophila*.

Supplemental material is available for this article.

Received May 6, 2016; revised version accepted June 15, 2016.

PIWI-interacting RNAs (piRNAs) form piRNA-induced silencing complexes (piRISCs) with PIWI proteins that repress transposons to maintain the integrity of the germline genome (Aravin et al. 2007; Brennecke et al. 2007; Ghildiyal and Zamore 2009; Juliano et al. 2011; Iwasaki et al. 2015). Somatic primary piRNA biogenesis in *Drosophila* has been extensively studied, mainly genetically and biochemically, using ovaries and a cultured ovarian somatic cell (OSC) line (Niki et al. 2006; Malone et al. 2009; Saito et al. 2009). According to the current model, piRNA precursors arising from piRNA clusters accumulate at specific granules, termed the Yb body and Dot COM, and are then processed at Yb bodies (Saito et al. 2010; Dennis et al. 2013; Murota et al. 2014). In parallel, Yb centralizes multiple primary piRNA factors to Yb bodies, including Armitage (Armi), Vreteno (Vret), Sister of Yb (SoYb), and Shutdown (Shu) (Iwasaki et al. 2015). Yb bodies are often surrounded by mitochondria (Murota et al. 2014). This unique spatial arrangement in the cytoplasm

enables Zucchini (Zuc), an endonuclease located on the surface of mitochondria with its active site facing the cytosol, to process piRNA intermediates into mature piRNAs (Ipsaro et al. 2012; Nishimasu et al. 2012). Primary piRNAs form piRISCs with Piwi but not with the other PIWI members Aub and AGO3 because of their absence in somatic cells. Piwi-piRISCs translocated to the nucleus transcriptionally repress transposons (Iwasaki et al. 2015).

Germ cells in *Drosophila* express Aub, AGO3, and Piwi (Saito et al. 2006; Brennecke et al. 2007; Gunawardane et al. 2007; Nishida et al. 2007). Of those, Aub and Piwi, but not AGO3, are loaded with primary piRNAs derived from piRNA clusters (Li et al. 2009; Malone et al. 2009). Piwi-piRISCs are then transported to the nucleus, where they repress transposons transcriptionally. In contrast, Aub-piRISCs remain in the cytoplasm and repress transposons by cleaving their mRNAs in a slicer-dependent manner. This Aub slicer-dependent RNA cleavage gives rise to secondary piRNAs, which are loaded onto AGO3. Aub-piRISCs and AGO3-piRISCs then operate a slicer-dependent feed-forward loop termed the ping-pong cycle, yielding a substantial amount of secondary piRNAs (Brennecke et al. 2007; Gunawardane et al. 2007). However, the detailed mechanism of the germ-specific process remains poorly understood, largely because an ex vivo *Drosophila* model system amenable to biochemical analyses has not been available. BmN4 cells (Kawaoka et al. 2009) have been used to study the mechanism underlying the ping-pong cycle but are of lepidopteran origin. BmN4 cells express two PIWI members but lack a homolog of *Drosophila* Piwi.

In *Drosophila*, mutations in *lethal (3) malignant brain tumor [l(3)mbt]* generate malignant brain tumors with metastatic potential (Gateff et al. 1993; Janic et al. 2010) due to deregulation of *l(3)mbt* signature (MBTS) genes (Janic et al. 2010). Multiple MBTS genes encode proteins with germline functions, and mutations in these genes (for instance, *piwi*) rescue the brain tumor phenotype (Janic et al. 2010). MBTS genes with germline functions include ping-pong factors such as *aub* and *vasa* (Janic et al. 2010). A few small RNAs in *l(3)mbt* mutant brain tumors were annotated as piRNAs (Janic et al. 2010). These findings of *l(3)mbt* mutations resulting in ectopic acquisition of germline traits in the brain prompted us to examine whether depletion of *l(3)mbt* in OSCs initiates the ping-pong cycle and causes the accumulation of secondary piRNAs in cells.

In this study, we found that both RNAi- and CRISPR-mediated loss of function of *l(3)mbt* lead to ectopic expression of Aub, AGO3, and Vasa—the core factors necessary for operating the germ-specific ping-pong cycle—in OSCs. Deep sequencing and comparison of mRNAs in the CRISPR-mediated mutant OSCs (Δ mbt-OSCs) and parental OSCs revealed that other ping-pong factors such as *qin* were up-regulated in Δ mbt-OSCs. Both Aub and AGO3 copurified with piRNAs in Δ mbt-OSCs. Deep sequencing these small RNA populations demonstrated that Aub- and AGO3-bound piRNAs show a typical ping-pong signature. Perinuclear foci resembling nuage,

[**Keywords:** piRNA; PIWI; ping-pong cycle; *l(3)mbt*; CRISPR; *Drosophila*]

³These authors contributed equally to this work.

Corresponding author: siomim@bs.s.u-tokyo.ac.jp

Article is online at <http://www.genesdev.org/cgi/doi/10.1101/gad.283929.116>. Freely available online through the *Genes & Development* Open Access option.

© 2016 Sumiyoshi et al. This article, published in *Genes & Development*, is available under a Creative Commons License (Attribution 4.0 International), as described at <http://creativecommons.org/licenses/by/4.0/>.

the ping-pong center (Brennecke et al. 2007; Gunawardane et al. 2007; Lim and Kai 2007; Malone et al. 2009), also appeared following *l(3)mbt* mutation. Depletion of Vasa in Δ mbt-OSCs disrupted the ping-pong pathway and Aub localization to the nuage-like structure. Use of Δ mbt-OSCs will greatly facilitate elucidation of the mechanism underlying secondary piRNA biogenesis and nuage formation in *Drosophila*.

Results and Discussion

Loss of l(3)mbt leads to ectopic expression of ping-pong factors in OSCs

OSCs express *l(3)mbt* (<http://flybase.org/reports/FBfr0221009.html>). We therefore treated OSCs with *l(3)mbt* siRNA duplexes (Supplemental Fig. S1A). The mRNA level of *l(3)mbt* was significantly decreased upon RNAi treatment (Supplemental Fig. S1B). In contrast, *ago3* and *vasa* were significantly up-regulated after *l(3)mbt* siRNA treatment, while changes in the level of *piwi* mRNA were negligible (Supplemental Fig. S1B). Western blotting detected AGO3, Vasa, and Aub in the RNAi-treated cells, while the levels of Piwi, Yb, Armi, and Krimper (Krimp) (Saito et al. 2009; Iwasaki et al. 2015; Sato et al. 2015) remained unchanged (Supplemental Fig. S1C).

We next set out to ablate *l(3)mbt* function by editing the genome in OSCs using the CRISPR/Cas9 system. With reference to two mutant alleles, *l(3)mbt^{GM76}* and *l(3)mbt^{E2}* (Wismar et al. 1995; Yohn et al. 2003; Janic et al. 2010), small guide RNAs (sgRNAs) were designed to target exon 5, which contains MBT domains (Fig. 1A). The two mutant alleles have an effect on tumorigenesis in the fly brain (Wismar et al. 1995; Janic et al. 2010). A genomic PCR fragment amplified with a primer set flanking the sgRNA targeting sites was shortened after CRISPR/Cas9 treatment (Fig. 1B). Sequencing the fragment revealed that a 558-nucleotide (nt) deletion occurred at the gene locus (Fig. 1A). Full-length *l(3)mbt* mRNA was not detectable by quantitative RT-PCR (qRT-PCR) in the mutant cells (data not shown). We refer to these cells here as Δ mbt-OSCs.

Deep sequencing and comparison of mRNAs in Δ mbt-OSCs and the parental OSCs revealed that, in addition to *ago3* and *vasa*, other ping-pong factors such as *aub*, *qin*, *tapas*, and *tejas* (Specchia et al. 2010; Gangaraju et al. 2011; Czech et al. 2013; Handler et al. 2013; Patil et al. 2014; Iwasaki et al. 2015) were markedly up-regulated in Δ mbt-OSCs (Fig. 1C; Supplemental Fig. S2A). Western blotting confirmed increased levels of Aub, AGO3, and Vasa in Δ mbt-OSCs (Fig. 1D). The levels of Piwi and other piRNA factors examined, such as Yb and Armi (Iwasaki et al. 2015), were nearly identical between the two cell lines (Fig. 1D), although a few factors showed slight changes in their mRNA levels (Fig. 1C; Supplemental Fig. S2A). Germ-specific genes tended to be more sensitive to loss of *l(3)mbt* than germ + soma and soma-specific genes (Fig. 1C; Supplemental Fig. S2A). The appearance of Yb in Δ mbt-OSCs suggests that CRISPR-mediated *l(3)mbt* loss had little effect on the elimination of somatic traits from the mutant cells. Focusing on MBTS genes revealed that many, if not all, were up-regulated in Δ mbt-OSCs (Supplemental Fig. S2B). Among non-MBTS genes that are up-regulated by mutations in *mbt* genes other than MBTS (Janic et al. 2010), the highest up-regulation

was observed for *ago3* (21.5-fold in Δ mbt-OSCs). Results of transcriptome-wide analysis are summarized in Supplemental Tables S1 and S2. We confirmed that loss of *l(3)mbt* had very little effect on the proliferation rate of OSCs (Supplemental Fig. S2C).

Loss of l(3)mbt activates the ping-pong cycle in OSCs

To compare Piwi-piRNA loading between Δ mbt-OSCs and OSCs, Piwi was immunoprecipitated from both lines, and extracted RNAs were ³²P-labeled. piRNAs copurified with Piwi similarly from both cell lines (Fig. 2A). We then deep-sequenced Piwi-bound piRNAs in Δ mbt-OSCs and compared the reads with those from OSCs (Fig. 2B–D; Supplemental Fig. S3A–D; Saito et al. 2009). This revealed that both sets of piRNAs show strong bias toward 1U and antisense orientation. The levels piRNAs from Δ mbt-OSCs and parental OSCs mapped to each transposon were highly similar ($R^2 = 0.872$). piRNAs were mapped similarly to *flamenco* (*flam*), a soma-specific single-strand piRNA cluster; *traffic jam* (*tj*), a genic piRNA source; and transposons such as *mdg1* (Brennecke et al. 2007; Malone et al. 2009; Robine et al. 2009; Saito et al. 2009). piRNAs corresponding to *42AB*, a germ-specific dual-strand piRNA cluster (Brennecke et al. 2007; Malone et al. 2009), were not contained in Piwi-bound piRNAs. This was expected because a component of the Rhino-Deadlock-Cutoff (RDC) complex, *cutoff*, which is necessary for producing piRNAs from *42AB* and other germ-specific dual-strand piRNA clusters (Mohr et al. 2014; Zhang et al. 2014), was undetected in both OSC lines (Supplemental Fig. S2A). Another component, *rhino*, whose expression was as low as *ago3* in OSCs, was even lower in Δ mbt-OSCs, while *deadlock* was expressed moderately in both OSCs and Δ mbt-OSCs (Supplemental Fig. S2A).

In Δ mbt-OSCs, both Aub and AGO3 copurified with piRNAs (Fig. 2E). Deep sequencing these small RNA populations clarified that Aub-bound and AGO3-bound piRNAs show distinct features (Fig. 2B–D; Supplemental Fig. S3A–D). While Aub-piRNAs showed significant nucleotide bias toward 1U and were mostly antisense, AGO3-piRNAs had strong 10A and sense biases. The correlation between levels of Piwi-bound and AGO3-bound piRNAs mapped to each transposon was low ($R^2 = 0.149$), while the correlation was significantly high between levels of Piwi-bound and Aub-bound piRNAs ($R^2 = 0.874$). Both *flam*-piRNAs and *tj*-piRNAs were found with Aub but not with AGO3. *42AB*-piRNAs were not detected with Aub or AGO3. Additionally, plotting the distribution of Aub-bound and AGO3-bound piRNAs to transposons *DM412*, *DM297*, and *mdg1* indicated the production of piRNAs from the same coordinate but in the opposite orientation.

We previously showed that both Myc-Aub and Myc-AGO3 exogenously expressed in OSCs by transfection are loaded with primary piRNAs, including *flam*-piRNAs and *tj*-piRNAs, which are normally loaded onto endogenous Piwi (Olivieri et al. 2012; Sato et al. 2015). This emphasized the compatibility of AGO3 with primary piRNA loading. However, in Δ mbt-OSCs, AGO3 avoided binding primary piRNAs; this was especially apparent when *tj*-piRNAs were compared (Supplemental Fig. S3C; Sato et al. 2015). In OSCs, Krimp sequesters unloaded AGO3 to Krimp bodies and blocks AGO3-primary piRNA loading (Olivieri et al. 2012; Sato et al. 2015). Krimp is crucial

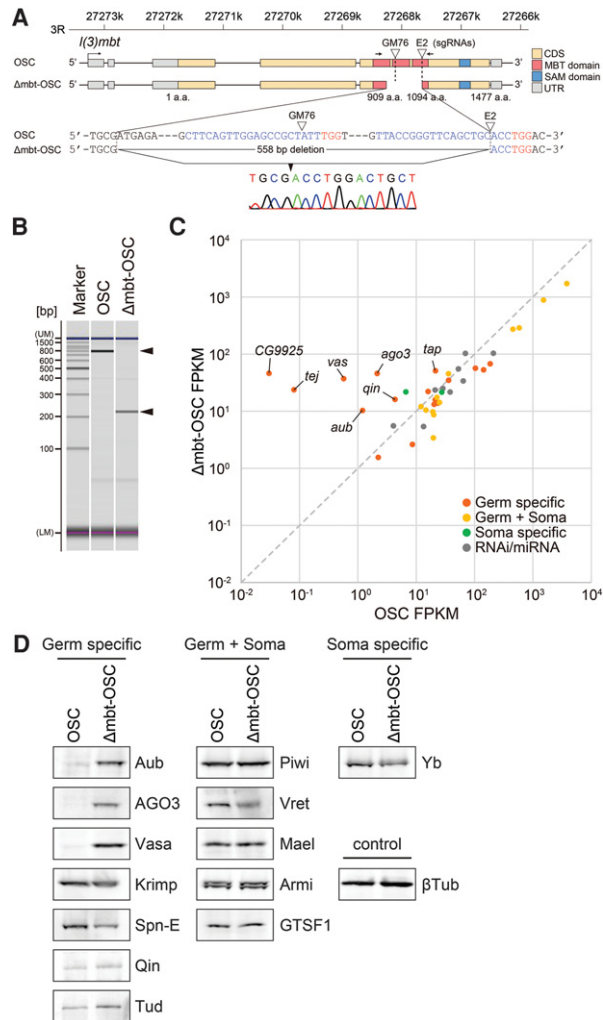


Figure 1. CRISPR-mediated generation of Δ mbt-OSCs. (A) Genomic structure of *I(3)mbt* in OSCs and Δ mbt-OSCs. sgRNAs GM76 and E2 targeting *I(3)mbt* exon 5 are indicated by arrowheads. Sequences at the *I(3)mbt* gene locus in OSCs and Δ mbt-OSCs are also shown (sgRNA and PAM sequences are shown in blue and red, respectively). (CDS) Protein-coding DNA sequence; (MBT domain) malignant brain tumor domain; (SAM domain) sterile α motif domain; (UTR) untranslated region. (B) Genomic PCR fragments amplified with a primer set, shown by arrows in A, are indicated by arrowheads (OSC, 772 nt; Δ mbt-OSC, 214 nt). (UM) Upper marker; (LM) lower marker. (C) Scatter plot comparing transcript abundance (mRNA-seq) of small RNA biogenesis factors in OSCs and Δ mbt-OSCs. Classification of the factors to four clades—germ-specific, germ + soma, soma-specific, and RNAi/miRNA—was carried out with reference to Handler et al. (2013). (FPKM) Fragments per kilobase of exon per million mapped sequence reads. (D) Western blotting shows protein levels of piRNA factors in OSCs and Δ mbt-OSCs. β Tubulin (β Tub) was detected as a loading control.

for AGO3 function in ovary germ cells (i.e., symmetrical dimethyl arginine [sDMA] modification and secondary piRNA association) (Sato et al. 2015; Webster et al. 2015); therefore, it would be expected that, in Δ mbt-OSCs, AGO3 loading with secondary piRNAs might be under the control of Krimp. Indeed, AGO3 was sDMA-modified in Δ mbt-OSCs, as in ovaries, while Myc-AGO3 in OSCs was sDMA-free (Fig. 2F; Supplemental Fig. S3E). However, this does not exclude the possibility that

unknown proteins other than Krimp may also be involved in the regulation of AGO3 sDMA modification along with Krimp.

If AGO3-bound piRNAs were produced via the ping-pong cycle in an Aub slicer-dependent manner, a ping-pong signal—i.e., complementary overlap of 10 nt at the 5' ends—should be observed between Aub-bound and AGO3-bound piRNAs. piRNA production by such a ping-pong cycle was evaluated, and a significant ping-pong signal was observed between Aub-bound and AGO3-bound piRNAs (Fig. 2G). These results, along with mapping data shown in Supplemental Figure S3D, further support the idea that AGO3-bound piRNAs are products of Aub slicer in the ping-pong pathway.

Piwi-bound primary piRNAs in OSCs involve a unique subset of piRNAs called phased piRNAs (Han et al. 2015; Mohn et al. 2015). Examination of piRNAs in Δ mbt-OSCs by focusing on this trait revealed that phased piRNAs with $d = 1$ (this means that two piRNAs can be mapped right next to each other on the same genomic strand without a nucleotide gap between them) are particularly abundant in Piwi-bound piRNAs ($Z_1 = 22.3$). This was comparable with Piwi-bound piRNAs ($Z_1 = 16.8$) in OSCs (Supplemental Fig. S4A,B). Z_1 scores of Aub-bound and AGO3-bound piRNAs in OSCs were 11.5 and 2.9, respectively (Supplemental Fig. S4A), suggesting that AGO3-bound piRNAs tend to exclude phased piRNAs (Han et al. 2015; Mohn et al. 2015). In contrast, piRNAs loaded onto Myc-AGO3 in OSCs (Sato et al. 2015) showed a significant phasing pattern ($Z_1 = 12.9$) (Supplemental Fig. S4C). These results further support the notion that AGO3 in Δ mbt-OSCs avoids binding primary piRNAs, in contrast to Myc-AGO3 in OSCs.

Appearance of perinuclear foci resembling nuage in Δ mbt-OSCs

Vasa, a germ-specific DEAD-box RNA helicase, plays a crucial role in the ping-pong cycle by displacing cleaved RNAs from Aub-piRISCs (or its counterpart, Siwi-piRISCs, in silkworms) in an ATP hydrolysis-dependent manner (Xiol et al. 2014; Nishida et al. 2015). Immunofluorescence in *Drosophila* ovaries showed that Aub, AGO3, and Vasa colocalize to nuage (Lim and Kai 2007; Malone et al. 2009; Iwasaki et al. 2015). Immunostaining of Δ mbt-OSCs revealed that Aub and Vasa mostly coincide at perinuclear foci that look similar to nuage (Fig. 3A). Myc-Aub exogenously expressed in OSCs was uniformly distributed in the cytosol and did not form speckles (Sato et al. 2015). Signals of Myc-Vasa in OSCs were slightly stronger at the perinuclear region in the cytoplasm but not punctate (Fig. 3B). Myc-Aub coexpressed with Vasa in OSCs was distributed almost evenly in the cytoplasm (Fig. 3B). These results suggest that some factors whose expression is up-regulated by loss of *I(3)mbt* function promote Aub to form nuage-like structures with Vasa in Δ mbt-OSCs.

Aub and AGO3 also colocalized to nuage-like structures (Fig. 3C). Krimp in OSCs sequesters unloaded AGO3 to Krimp bodies, which are generally present at a frequency of one per cell (Fig. 3D; Olivieri et al. 2012; Sato et al. 2015). However, in Δ mbt-OSCs, AGO3-positive foci were more numerous than one per cell, and some could be superimposed with Aub-positive foci. This led us to examine the cellular localization of Krimp in Δ mbt-OSCs,

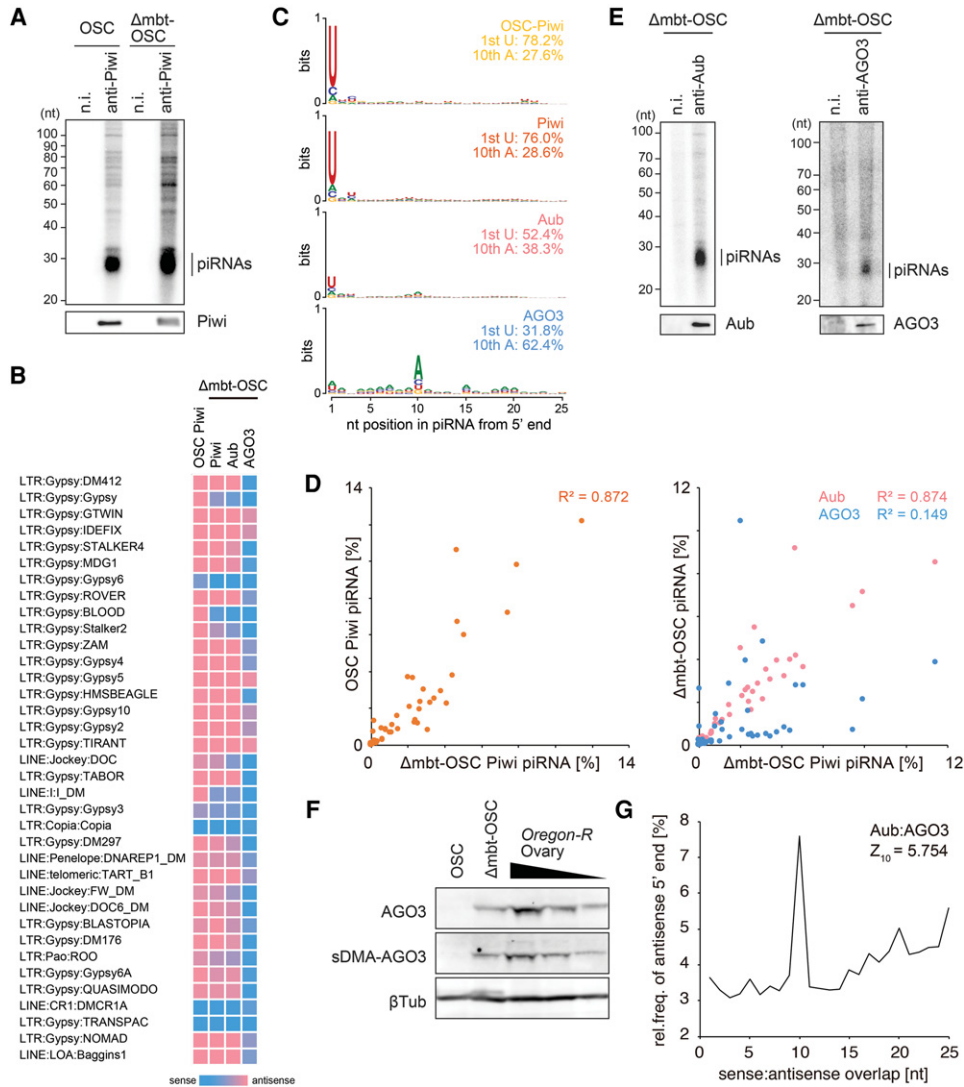


Figure 2. The ping-pong pathway in Δ mbt-OSCs. (A) 32 P-labeled piRNAs (top panel) associated with Piwi (bottom panel) in OSCs and Δ mbt-OSCs. (n.i.) Nonimmune IgG. (B) Heat maps of piRNA strand bias. Strand bias of transposon-derived piRNAs in Piwi/Aub/AGO3 small RNA libraries from Δ mbt-OSCs is shown. Strand bias of Piwi-bound piRNAs in parental OSCs (Ishizu et al. 2015) is also shown. (C) Sequence logos of Piwi/Aub/AGO3-bound piRNAs mapped to transposons in Δ mbt-OSCs. Sequence logos of Piwi-bound piRNAs in parental OSCs (Ishizu et al. 2015) are also shown (OSC Piwi at the top). (D, left) Scatter plot showing the correlation of antisense Piwi-bound piRNA reads in OSCs (percentage; Y-axis) with those in Δ mbt-OSCs (percentage; X-axis). (D, right) The correlation of antisense Aub-bound (pink dots) and antisense AGO3-bound (blue dots) piRNA reads in Δ mbt-OSCs (percentage; Y-axis) with antisense Piwi-bound piRNA reads in Δ mbt-OSCs (percentage; X-axis) is also shown. Each dot corresponds to the ratio of piRNAs mapped to transposons (shown in B). (E) 32 P-labeled piRNAs (top panel) associated with Aub and AGO3 (bottom panel) in Δ mbt-OSCs. (n.i.) Nonimmune IgG. (F) Western blotting shows that AGO3 in Δ mbt-OSCs is dimethylated, as in ovaries. (G) Depiction of the ping-pong signature between antisense Aub-bound piRNAs and sense AGO3-bound piRNAs, defined as the value at position 10 nt. Graphs indicate the relative frequency that a complementary piRNA exists with a 5' end (Y-axis) at the indicated distance (X-axis).

and we observed that co-localization of Krimp with AGO3 was apparent (Fig. 3D), as occurs in ovaries where Krimp normally accumulates at nuage. Krimp bodies are present only when piRNA biogenesis is defective because of mutations in piRNA factors such as *aub*. These results support the intriguing idea that Δ mbt-OSCs likely recapitulate formation of the ping-pong center.

We next examined the spatial relationship between Yb and Aub-positive structures in Δ mbt-OSCs. Aub and Yb signals only occasionally coincide (Fig. 3E), although the number of Yb bodies may be higher in Δ mbt-OSCs compared with that in OSCs. These results suggest that primary and secondary piRNA biogenesis pathways may occur

separately at Yb bodies and Aub-positive nuage-like foci, respectively, in Δ mbt-OSCs.

In *vasa* mutant ovaries, Aub does not accumulate in the nuage and is evenly distributed in the cytosol of nurse cells (Lim and Kai 2007; Malone et al. 2009; Iwasaki et al. 2015). We therefore asked how depletion of Vasa affects Aub localization in Δ mbt-OSCs. Treatment of Δ mbt-OSCs with *vasa* siRNA duplexes caused Aub to be largely dispersed in the cytosol (Fig. 4A,B). Under such conditions, AGO3 was loaded with far fewer piRNAs, although Aub piRNA association remained largely unaffected (Fig. 4C). Thus, Vasa depletion disrupted the ping-pong pathway in Δ mbt-OSCs, as expected.

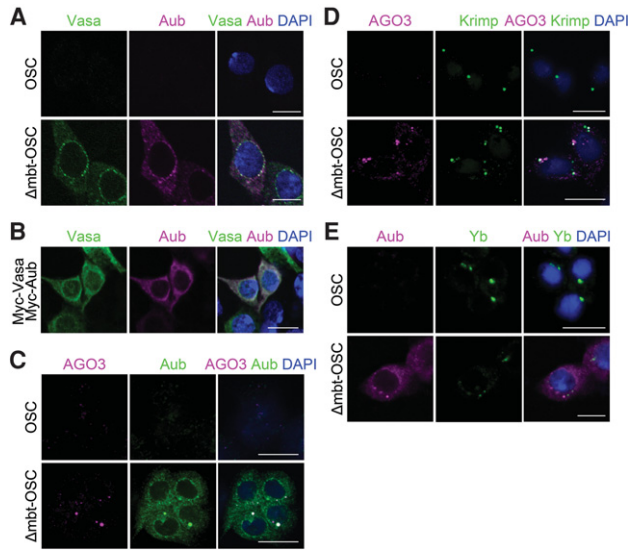


Figure 3. Nuage-like structures in Δmbt -OSCs. (A) Immunofluorescence shows that Aub and Vasa coincide at nuage-like structures in Δmbt -OSCs. (B) Coexpression of Myc-Aub with Myc-Vasa in OSCs by transfection. Immunofluorescence was performed using anti-Vasa and anti-Aub antibodies. (C) AGO3 colocalizes with Aub in Δmbt -OSCs. (D) AGO3 partially colocalizes with Krimp in Δmbt -OSCs. (E) Aub and Yb only occasionally coincide in Δmbt -OSCs. Bars, 10 μm .

Loss of *l(3)mbt* fails to activate the ping-pong cycle in S2 cells

The *Drosophila* cell line S2 is of embryonic and somatic origin; therefore, PIWI proteins and piRNAs are below detection levels (Saito et al. 2006, 2009). *l(3)mbt* mRNA was detected in S2 cells by qRT-PCR (data not shown); therefore, we examined whether *l(3)mbt* knockdown has an impact on piRNA production in S2 cells. Upon RNAi, Aub was slightly up-regulated (Fig. 4D). However, very low levels of other factors, including Piwi, AGO3, and Vasa, were detected (Fig. 4D). Indeed, we failed to determine PIWI-piRNA loading by immunoprecipitation (data not shown). Although *Drosophila* brains and S2 cells are both nongonadal and somatic, the mechanism by which *l(3)mbt* controls downstream genes in these cells seems to be distinct.

In summary, our results show that CRISPR-mediated *l(3)mbt* knockout in OSCs leads to the ectopic expression of ping-pong factors, resulting in the accumulation of secondary piRNAs that are otherwise undetected in OSCs. In the mutant cells, AGO3-loaded secondary piRNAs were mostly 10A-biased and sense-oriented (Fig. 2; Supplemental Fig. S3). piRNA mapping revealed that the piRNAs originate from transposon mRNAs (Supplemental Fig. S3D). However, Piwi was expressed in Δmbt -OSCs to an extent similar to that in parental OSCs (Fig. 2A). Piwi-bound piRNAs were highly comparable in the two cell lines in all aspects, including piRNA origins and nucleotide and strand biases (Fig. 2; Supplemental Fig. S3). Thus, Piwi in Δmbt -OSCs should be similarly functional in repressing transposons compared with Piwi in OSCs. Indeed, Piwi was localized in the nucleus in both Δmbt -OSCs and OSCs (Supplemental Fig. S5A). The levels of transposon mRNAs were not drastically changed by loss of *l(3)mbt* ($R^2 = 0.988$) (Supplemental Fig. S5B), suggesting

that *l(3)mbt* is dispensable in transposon silencing in ovarian somas. The question then arises of where transposon mRNAs that give rise to sense AGO3-bound piRNAs came from in Δmbt -OSCs. Our previous study showed that overexpression of Myc-Aub in OSCs caused a slight but significant increase in the levels of *mdg1* and *DM297*, which are targets of Piwi in OSCs (Sato et al. 2015). This derepression of transposons could be because Myc-Aub competes with endogenous Piwi for primary piRNAs, impairing the Piwi-mediated transcriptional silencing activity. Indeed, AGO3-bound piRNAs included piRNAs originating from *mdg1* and *DM297* mRNAs (Fig. 2B). These results raise the intriguing idea that both transcriptional and post-transcriptional transposon silencing (i.e., the ping-pong cycle) occur in Δmbt -OSCs, mediated by nuclear Piwi-piRNA and cytoplasmic Aub-piRNA complexes, respectively, as in germ cells in fly ovaries. Thus, this newly made cell line, Δmbt -OSC, is the first cell line of any animal that accommodates both transcriptional and post-transcriptional silencing events and hence would also be useful in exploring the relationship of the two pathways.

Materials and methods

Establishment of Δmbt -OSCs

Gene knockout in OSCs using the CRISPR/Cas9 system and isolation of knockout OSCs were performed essentially as described previously (Ishizu et al. 2015). In brief, OSCs were transfected with 0.2 μg of a plasmid expressing both pBS-Hsp70-Cas9 (Addgene, 46294) and the blasticidin resistance gene and 4 μg of two sgRNA-expressing plasmids (GM76 and E2) using Xfect transfection reagent (TaKaRa Clontech). After incubation for 24 h, blasticidin (Thermo Fisher Scientific, Inc., R210-01) was added to the culture medium at 50 $\mu g/mL$. The next day, 5.0×10^3 cells were passaged in 3.5-cm dishes and allowed to grow in blasticidin-containing medium. During culturing, cells were washed with the medium to remove nonadherent dead cells. After 6–7 d of culture, 5.0×10^3 cells were passaged in 6-cm dishes and allowed to grow in blasticidin-containing medium. After further incubation for a few days, colonies were picked and passaged in single wells of 24-well plates. The next day, these colonies were suspended with a Tip Strainer (Bel-Art) and allowed to grow to confluence. To detect the genomic deletion, genomic DNA was extracted using QuickExtract

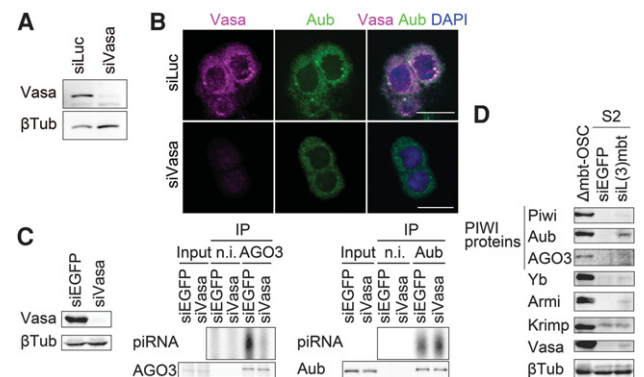


Figure 4. The effect of Vasa depletion in Δmbt -OSCs. (A) RNAi efficiently reduced the amount of Vasa in Δmbt -OSCs. siLuc was used as a negative control. (B) Depletion of Vasa in Δmbt -OSCs caused Aub to be scattered in the cytoplasm in Δmbt -OSCs. Bars, 10 μm . (C) AGO3, but not Aub, associates with fewer secondary piRNAs in Δmbt -OSCs upon Vasa RNAi treatment. siEGFP was used as a negative control. (n. i.) Nonimmune IgG. (D) Expression levels of piRNA factors in S2 cells upon *l(3)mbt* depletion by RNAi. dsEGFP (siEGFP) was used as a negative control.

DNA extraction solution (Epicenter) following the manufacturer's protocol, and the genomic region flanking the CRISPR target site was amplified by PCR and then analyzed using MultiNa (Shimadzu).

Acknowledgments

We thank D. Chen and T. Kai for providing antibodies. We also thank K.M. Nishida, A. Nagao, and H. Ohtani for producing antibodies, and the other members of the Siomi laboratories, particularly K. Saito and S. Yamanaka, for discussions and comments on the manuscript. We are also thankful to T. Ono and W. Iwasaki for bioinformatics assistance. This work was supported by a Grant-in-Aid for Scientific Research from the Ministry of Education, Culture, Sports, Science, and Technology of Japan to K.S., Y.W.I., H.S., and M.C.S.

References

- Aravin AA, Hannon GJ, Brennecke J. 2007. The Piwi-piRNA pathway provides an adaptive defense in the transposon arms race. *Science* **318**: 761-764.
- Brennecke J, Aravin AA, Stark A, Dus M, Kellis M, Sachidanandam R, Hannon GJ. 2007. Discrete small RNA-generating loci as master regulators of transposon activity in *Drosophila*. *Cell* **128**: 1089-1103.
- Czech B, Preall JB, McGinn J, Hannon GJ. 2013. A transcriptome-wide RNAi screen in the *Drosophila* ovary reveals factors of the germline piRNA pathway. *Mol Cell* **50**: 749-761.
- Dennis C, Zanni V, Brasset E, Eymery A, Zhang L, Mteirek R, Jensen S, Rong YS, Vaury C. 2013. 'Dot COM,' a nuclear transit center for the primary piRNA pathway in *Drosophila*. *PLoS One* **8**: e72752.
- Gangaraju VK, Yin H, Weiner MM, Wang J, Huang XA, Lin H. 2011. *Drosophila* Piwi functions in Hsp90-mediated suppression of phenotypic variation. *Nat Genet* **43**: 153-158.
- Gateff E, Löffler T, Wismar J. 1993. A temperature-sensitive brain tumor suppressor mutation of *Drosophila melanogaster*: developmental studies and molecular localization of the gene. *Mech Dev* **41**: 15-31.
- Ghildiyal M, Zamore PD. 2009. Small silencing RNAs: an expanding universe. *Nat Rev Genet* **10**: 94-108.
- Gunawardane LS, Saito K, Nishida KM, Miyoshi K, Kawamura Y, Nagami T, Siomi H, Siomi MC. 2007. A slicer-mediated mechanism for repeat-associated siRNA 5' end formation in *Drosophila*. *Science* **315**: 1587-1590.
- Han BW, Wang W, Li C, Weng Z, Zamore PD. 2015. piRNA-guided transposon cleavage initiates Zucchini-dependent, phased piRNA production. *Science* **348**: 817-821.
- Handler D, Meixner K, Pizka M, Lauss K, Schmied C, Gruber FS, Brennecke J. 2013. The genetic makeup of the *Drosophila* piRNA pathway. *Mol Cell* **50**: 762-777.
- Ipsaro JJ, Haase AD, Knott SR, Joshua-Tor L, Hannon GJ. 2012. The structural biochemistry of Zucchini implicates it as a nuclease in piRNA biogenesis. *Nature* **491**: 279-283.
- Ishizu H, Iwasaki YW, Hirakata S, Ozaki H, Iwasaki W, Siomi H, Siomi MC. 2015. Somatic primary piRNA biogenesis driven by cis-acting RNA elements and trans-acting Yb. *Cell Rep* **12**: 429-440.
- Iwasaki YW, Siomi MC, Siomi H. 2015. PIWI-interacting RNA: its biogenesis and functions. *Annu Rev Biochem* **84**: 405-433.
- Janic A, Mendizabal L, Llamazares S, Rossell D, Gonzalez C. 2010. Ectopic expression of germline genes drives malignant brain tumor growth in *Drosophila*. *Science* **330**: 1824-1827.
- Juliano C, Wang J, Lin H. 2011. Uniting germline and stem cells: the function of Piwi proteins and the piRNA pathway in diverse organisms. *Annu Rev Genet* **45**: 447-469.
- Kawaoka S, Hayashi N, Suzuki Y, Abe H, Sugano S, Tomari Y, Shimada T, Katsuma S. 2009. The *Bombix* ovary-derived cell line endogenously expresses PIWI/PIWI-interacting RNA complexes. *RNA* **15**: 1258-1264.
- Li C, Vagin VV, Lee S, Xu J, Ma S, Xi H, Seitz H, Horwich MD, Syrzycka M, Honda BM, et al. 2009. Collapse of germline piRNAs in the absence of Argonaute3 reveals somatic piRNAs in flies. *Cell* **137**: 509-521.
- Lim AK, Kai T. 2007. Unique germ-line organelle, nuage, functions to repress selfish genetic elements in *Drosophila melanogaster*. *Proc Natl Acad Sci* **104**: 6714-6719.
- Malone CD, Brennecke J, Dus M, Stark A, McCombie WR, Sachidanandam R, Hannon GJ. 2009. Specialized piRNA pathways act in germline and somatic tissues of the *Drosophila* ovary. *Cell* **137**: 522-535.
- Mohn F, Sienski G, Handler D, Brennecke J. 2014. The rhino-deadlock-cutoff complex licenses noncanonical transcription of dual-strand piRNA clusters in *Drosophila*. *Cell* **157**: 1364-1379.
- Mohn F, Handler D, Brennecke J. 2015. piRNA-guided slicing specifies transcripts for Zucchini-dependent, phased piRNA biogenesis. *Science* **348**: 812-817.
- Murota Y, Ishizu H, Nakagawa S, Iwasaki YW, Shibata S, Kamatani MK, Saito K, Okano H, Siomi H, Siomi MC. 2014. Yb integrates piRNA intermediates and processing factors into perinuclear bodies to enhance piRISC assembly. *Cell Rep* **8**: 103-113.
- Niki Y, Yamaguchi T, Mahowald AP. 2006. Establishment of stable cell lines of *Drosophila* germ-line stem cells. *Proc Natl Acad Sci* **103**: 16325-6330.
- Nishida KM, Saito K, Mori T, Kawamura Y, Nagami-Okada T, Inagaki S, Siomi H, Siomi MC. 2007. Gene silencing mechanisms mediated by Aubergine piRNA complexes in *Drosophila* male gonad. *RNA* **13**: 1911-1922.
- Nishida KM, Iwasaki YW, Murota Y, Nagao A, Mannen T, Kato Y, Siomi H, Siomi MC. 2015. Respective functions of two distinct Siwi complexes assembled during PIWI-interacting RNA biogenesis in *Bombix* germ cells. *Cell Rep* **10**: 193-203.
- Nishimasu H, Ishizu H, Saito K, Fukuhara S, Kamatani MK, Bonnefond L, Matsumoto N, Nishizawa T, Nakanaga K, Aoki J, et al. 2012. Structure and function of Zucchini endoribonuclease in piRNA biogenesis. *Nature* **491**: 284-287.
- Olivieri D, Senti KA, Subramanian S, Sachidanandam R, Brennecke J. 2012. The cochaperone shutdown defines a group of biogenesis factors essential for all piRNA populations in *Drosophila*. *Mol Cell* **47**: 954-969.
- Patil VS, Anand A, Chakrabarti A, Kai T. 2014. The Tudor domain protein Tapas, a homolog of the vertebrate Tdrd7, functions in the piRNA pathway to regulate retrotransposons in germline of *Drosophila melanogaster*. *BMC Biol* **12**: 61.
- Robine N, Lau NC, Balla S, Jin Z, Okamura K, Kuramochi-Miyagawa S, Blower MD, Lai EC. 2009. A broadly conserved pathway generates 3'UTR-directed primary piRNAs. *Curr Biol* **19**: 2066-2076.
- Saito K, Nishida KM, Mori T, Kawamura Y, Miyoshi K, Nagami T, Siomi H, Siomi MC. 2006. Specific association of Piwi with rasirRNAs derived from retrotransposon and heterochromatic regions in the *Drosophila* genome. *Genes Dev* **20**: 2214-2222.
- Saito K, Inagaki S, Mituyama T, Kawamura Y, Ono Y, Sakota E, Kotani H, Asai K, Siomi H, Siomi MC. 2009. A regulatory circuit for piwi for the large *Maf* gene traffic jam in *Drosophila*. *Nature* **461**: 1296-1299.
- Saito K, Ishizu H, Komai M, Kotani H, Kawamura Y, Nishida KM, Siomi H, Siomi MC. 2010. Roles for the Yb body components Armitage and Yb in primary piRNA biogenesis in *Drosophila*. *Genes Dev* **24**: 2493-2498.
- Sato K, Iwasaki YW, Shibuya A, Carninci P, Tsuchizawa Y, Ishizu H, Siomi MC, Siomi H. 2015. Krimper enforces an antisense bias on piRNA pools by binding AGO3 in the *Drosophila* germline. *Mol Cell* **59**: 553-563.
- Specchia V, Piacentini L, Tritto P, Fanti L, D'Alessandro R, Palumbo G, Pimpinelli S, Bozzetti MP. 2010. Hsp90 prevents phenotypic variation by suppressing the mutagenic activity of transposons. *Nature* **463**: 662-665.
- Webster A, Li S, Hur JK, Wachsmuth M, Bois JS, Perkins EM, Patel DJ, Aravin AA. 2015. Aub and Ago3 are recruited to nuage through two mechanisms to form a ping-pong complex assembled by Krimper. *Mol Cell* **59**: 564-575.
- Wismar J, Löffler T, Habtemichael N, Vef O, Geissen M, Zirwes R, Altmeier W, Sass H, Gateff E. 1995. The *Drosophila melanogaster* tumor suppressor gene *lethal(3)malignant brain tumor* encodes a proline-rich protein with a novel zinc finger. *Mech Dev* **53**: 141-154.
- Xiol J, Spinelli P, Laussmann MA, Homolka D, Yang Z, Cora E, Couté Y, Conn S, Kadlec J, Sachidanandam R, et al. 2014. RNA clamping by Vasa assembles a piRNA amplifier complex on transposon transcripts. *Cell* **157**: 1698-1711.
- Yohn CB, Pusateri L, Barbosa V, Lehmann R. 2003. *l(3)malignant brain tumor* and three novel genes are required for *Drosophila* germ-cell formation. *Genetics* **165**: 1889-1900.
- Zhang Z, Wang J, Schultz N, Zhang F, Parhad SS, Tu S, Vreven T, Zamore PD, Weng Z, Theurkauf WE. 2014. The HP1 homolog rhino anchors a nuclear complex that suppresses piRNA precursor splicing. *Cell* **157**: 1353-1363.